UCRL-17628

cy. 2

University of California

Ernest O. Lawrence Radiation Laboratory

HIGH TEMPERATURE VAPORIZATION MECHANISMS

Gabor A. Somorjai

June 1967

Berkeley, California

DISCLAIMER

Submitted to: Third International Symposium
High Temperature Technology,
Asilomar, Calif., Sept. 17-20, 1967.

UCRL-17628
Preprint

UNIVERSITY OF CALIFORNIA

Lawrence Radiation Laboratory
Berkeley, California

AEC Contract No. W-7405-eng-48

HIGH TEMPERATURE VAPORIZATION MECHANISMS

Gabor A. Somorjai

June 1967

HIGH TEMPERATURE VAPORIZATION MECHANISMS

Gabor A. Somorjai

Inorganic Materials Research Division, Lawrence Radiation Laboratory,
and Department of Chemistry, University of California,
Berkeley, California

ABSTRACT

Experimental information about the vaporization mechanism of solids is obtained from evaporation rate measurements which are carried out far from equilibrium. In such studies one stable face of a single crystal should be used. Vacuum evaporation rates of solids which undergo structural rearrangement, dissociation or association upon vaporization are, in general, markedly lower ($\alpha \ll 1$) than the maximum evaporation rate ($\alpha = 1$) predicted by the Hertz-Knudsen-Langmuir equation. The rate controlling step in the vaporization process, in most cases, is a surface reaction followed by the rapid desorption of the vaporizing species. It is expected that most refractory compounds (carbides, oxides, borides and nitrides) can have vacuum evaporation rates which are several orders of magnitude lower than the maximum rate derived from equilibrium studies. Several mechanisms leading to congruent and non-congruent vaporization are discussed. The vaporization characteristics of the different groups of refractory solids are summarized. Experiments are suggested to elucidate the mechanism of vaporization of refractory materials.

INTRODUCTION

The vaporization characteristics of solids are studied, in general, under two distinctly different experimental conditions: (a) equilibrium vaporization studies in which the vapor pressure and the vapor composition are determined, and from which may be determined other important thermodynamic data.[1] These equilibrium experiments, however, do not give information about the reaction path, i.e., the evaporation mechanism by which the solid constituents break away from their lattice sites and desorb from the surface. (b) Investigations of the kinetics of vaporization are carried out far from equilibrium, most frequently in vacuum.[2] Vacuum vaporization (Langmuir vaporization) experiments are commonly used in high temperature chemistry. It is well established[3,4] that evaporation is a multistep process during which the vaporizing atoms may undergo surface rearrangements or diffusion controlled reactions prior to the desorption step.

Under conditions of vacuum vaporization the evaporation rate is determined by the particular reaction step which is the slowest of the series of reaction steps leading to the desorption of the vaporizing species.[2] On the other hand, the evaporation rate from an equilibrium source (effusion cell) and the vapor composition of the solid in equilibrium with its vapor is determined by the thermodynamics of the system. The conditions required for the two rates to be equal are so stringent (to be shown later) that they can rarely be met. The evaporation rates (moles/cm^2sec) of solids into vacuum are generally smaller than their evaporation rates (moles/cm^2sec) from an equilibrium source at a given temperature. For diatomic or polyatomic solids there can be several

orders of magnitude difference between the two rates if the solid undergoes dissociation or association upon evaporation.[2] Thus, if technology calls for sustained performance of a material at high temperatures and in vacuum it should be recognized that most materials will vaporize appreciably slower than might be deduced from the vapor pressure data obtained by equilibrium measurements.

In this paper we shall describe in some detail studies which are carried out to uncover the evaporation mechanisms of compounds in the IA-VIIA, IIB-VIA, and IIIA-VA groups of the periodic table. We have studied the evaporation mechanism of cadmium sulfide single crystals[5,6] and studies of sodium chloride and gallium arsenide crystals are in progress. We shall discuss several other evaporation mechanisms which have been investigated and we shall attempt to correlate the kinetic data, whenever possible, with the evaporation characteristics of carbides, nitrides, borides, oxides and silicides. Experiments will be suggested to further elucidate the vaporization mechanism of different groups of refractory compounds.

We shall discuss the evaporation kinetics of solids only under vacuum vaporization conditions. In the presence of reacting gases, in either oxidizing or reducing atmospheres the rates of removal of the solid can be altered drastically due to the chemical reactions which take place at the interface. The rate limiting vaporization step might be different under these conditions from that in vacuum.

PRINCIPLES OF VAPORIZATION KINETICS STUDIES

Consider the vaporization of one face of a single crystal of a monatomic solid, (A). Its net evaporation rate, J_v, may be written as

$$J_v(\text{moles/cm}^2\text{sec}) = k\,A(\text{solid}) - k'\,A\,(\text{vapor}) \qquad (1)$$

where k and k' are the overall rate constants of the multistep evaporation and condensation reactions, respectively, A(solid) and A(vapor) are the surface and vapor concentrations. In order to achieve a steady state rate of vaporization the surface concentration, A(solid), and thus, the surface area of the crystal should remain constant during evaporation. It should be noted that due to this criterion different crystal faces may also have different vaporization rates.[2]

If the vaporization is carried out in vacuum so that the vapor atoms cannot return to the vaporizing surface the evaporation rate is given by $J_v = k\,A(\text{solid})$. It is customary for historical reasons to express the evaporation rate in terms of the condensation rate. This can be done only in equilibrium where the two rates are equal. Thus, in equilibrium, $k\,A(\text{solid})^{eq} = k'\,A(\text{vapor})^{eq} = P_{eq}\,(2\pi MRT)^{-1/2}$, or

$$J_{max}(\text{moles/cm}^2\text{sec}) = P_{eq}(2\pi MRT)^{-1/2} \qquad (2)$$

where P_{eq} is the equilibrium vapor pressure and all other symbols have their usual meaning. This expression gives the maximum evaporation rate, J_{max}, of the monatomic solid in equilibrium. The atomic weight, M, should be replaced by an average molecular weight $\bar{M}$, in case there are

more than one vaporizing species ($\bar{M} = \sum_i n_i M_i / \sum_i n_i$ where n_i and M_i are, respectively, the number of molecules and the molecular weight of the i^{th} species). Although Eq. (2) has been derived for the vaporization or condensation rates near equilibrium it is frequently used to correlate evaporation rates with vapor pressure data when the experiment was carried out far from equilibrium. Any deviation from this maximum rate due to the different experimental conditions is then taken into account by the insertion of α, the evaporation coefficient, into Eq. (2)

$$J_v(\text{moles/cm}^2\text{sec}) = k(A)\text{solid} = \alpha P_{eq}(2\pi MRT)^{-1/2} \qquad (3)$$

The evaporation coefficient can thus be defined as $\alpha(T) = J_v(T)/J_{max}(T)$, the ratio of the observed evaporation rate, J_v, and the maximum rate in equilibrium, J_{max}, at a given temperature.

Consider now the physical model which would lead to $\alpha = 1$, a condition which is frequently evoked in vaporization studies. It requires that every surface atom should be available for vaporization, and that the activation enthalpy of vaporization, ΔH^*, be equal to the enthalpy of sublimation, ΔH_v^o. Furthermore, the vaporization of surface atoms should take place from sites which are indistinguishable and in which their internal states are identical to that of atoms already in the gas phase.[2,4]

These conditions can rarely be met for most solids. It is well established that the surface is heterogeneous, the surface atoms or molecules have different binding energies at different surface sites[7] and can have different internal partition function. Thus, only a fraction of all surface species may have a binding energy equal to ΔH_v^o.

Solids which undergo rearrangements,[4] association, or dissociation,[2] or even a change in bond length would exhibit evaporation rates which are lower than the maximum rate. Only molecular solids which have strong bonds within the molecular units and only weak dispersion forces between the molecules would be expected to vaporize with a maximum rate. Metals which vaporize mostly as monatomic species often have maximum evaporation rates.[3,8] This is somewhat surprising since metal atoms in the crystal lattice have strong and long range electronic interactions with neighbors. Thus, metal atoms in the surface have physical-chemical properties which are markedly different from those in the vapor. More studies using single crystal surfaces should be carried out to explore the reasons for their high vaporization rate.

Equation (3) and the definition of α ($\alpha(T) = J_v(T)/J_{max}(T)$) show that the evaporation coefficient should be temperature dependent since it is also proportional to the rate constant of the vaporization reaction. In essence, when Eq. (3) is used to describe the evaporation process, all of the experimental information concerning the evaporation mechanism is hidden in the value of the evaporation coefficients. Therefore, α is very sensitive to almost any change in the conditions of the vaporization experiment. Thus it is more useful to express the evaporation rate, far from equilibrium, in terms of a rate equation [$J_v = k(A)_{solid}$]. By changing the conditions of vaporization the reaction steps of the multi-step evaporation reaction can be uncovered and the rate constant of the rate limiting step may be determined.

In order to determine the detailed mechanism of vaporization of a given substance one may begin with the determination of the activation enthalpy, ΔH_v^*. This datum is obtained from the temperature dependence

of the vacuum evaporation rate using a single crystal surface. If there is congruent vaporization, i.e., the composition of the solid remains virtually unchanged in the studied temperature range,[2] the logarithm of the rate plotted against $1/T^{\circ}K$ should give a straight line. The slope of this line can be used to calculate an activation enthalpy which may then be compared with the enthalpy of vaporization, ΔH_v^o. A value of $\Delta H_v^* \neq \Delta H_v^o$ indicates that the rate limiting step is other than the desorption of mobile adatoms from the surface into vacuum.[2] It should be noted that ΔH_v^* can be larger or smaller for the rate limiting surface step than the heat of sublimation since the rate of the slow reaction step depends on the product, $k''(A)^*$ and not on k" alone where k" is the rate constant of the rate controlling step and $(A)^*$ is the surface concentration of species with adequate energy to participate in the rate determining reaction step. Thus, even if $\Delta H_v^* < \Delta H_v^o$, either the surface concentration $(A)^*$ or the pre-exponential factor ($k'' = A_o e^{-\Delta H^*/RT}$) might be small and can make the particular reaction step rate controlling.[2]

A noncongruent vaporization process may easily be recognized by the marked time dependence of the evaporation rate at a given temperature. When the composition of the solid changes during vaporization, a steady state evaporation rate cannot be established. For some of the noncongruently vaporizing solids a steady state vaporization rate may be achieved after an "induction period" as will be discussed later. For these substances an activation enthalpy, ΔH_v^*, may also be determined from the temperature dependence of the steady state rates.

The knowledge of the activation enthalpy alone, however, does not reveal the detailed mechanism of vaporization.[2] Complimentary experiments should be performed to uncover the reaction steps leading to the desorption

of the vaporizing species. Here we list some of the experiments which under proper conditions were found useful in identifying the reaction steps of complex vaporization reactions.

1. Vaporization rate measurements using single crystals which are doped with (a) one of the crystal constituents,[9,10] (b) impurities,[11] and (c) crystal defects in excess of their steady state concentration.[10,12]

2. Evaporation rate measurements as a function of the surface concentration of the vaporizing species.[6]

3. Studies of the vapor composition over freely vaporizing solid and its variation as equilibrium is approached.[13]

4. Measurement of the evaporation rates in a temperature range where phase transitions (melting) occur.[14]

5. Study of the variation of the solid composition under different vaporization conditions.[10,15]

6. Study of the effect of liquid catalysts on the evaporation rate.[16,17]

7. Illumination of the vaporizing surface by light of suitable wavelength and intensity.[9,18]

EXPERIMENTAL CONSIDERATIONS IN STUDIES OF VAPORIZATION MECHANISMS

In order to obtain reproducible evaporation rates a "stable" face of a single crystal of well-defined surface area should be used. A "stable" face remains unchanged under vacuum evaporation conditions while an unstable face shows faceting, i.e., new crystal faces develop during vaporization with a corresponding uncontrolled variation of the surface area.[19] The difficulties in carrying out experiments using polycrystalline powders and in interpreting the results of the evaporation rate studies have

been discussed recently.[20] The surface area of powders is unknown and irreproducible and the crevices and channels between the particles can act as small effusion cells in which the vapor atoms may undergo many collisions before leaving the solid. Thus, a certain fraction of the powder surface acts as an equilibrium source and the measured overall evaporation rate will fall between the true vacuum evaporation rate and the maximum (equilibrium) evaporation rate.

A typical single crystal surface area of 0.1 cm^2 was found to give reproducible results in the rate studies.[2] Samples of appreciably larger size may vaporize unevenly due to a temperature gradient along the crystal surface. For smaller samples the error due to that fraction of atoms which vaporize from other crystal faces (no matter how well they are masked) becomes increasingly larger.

The composition of polyatomic solids may change as a function of the thermal history of the samples.[15] In addition, for both monatomic and polyatomic solids the surface topology (concentrations of steps, kinks, ...) can be a strong function of the thermal history and purity of the crystals which are used in the vaporization studies. In semiconductors or insulators the concentration of charge carriers may vary drastically with minute changes of impurity or defect concentrations. Therefore it is important to use uniformly high purity samples which are subjected to uniform annealing processes to standardize the surface and bulk physical properties. Annealing, in general, should be carried out in the temperature range of the evaporation studies.

Vaporization is an endothermic reaction and excessive heat loss due to rapid sublimation may result in surface cooling.[21] This can be avoided

by restricting the evaporation rate measurements to small vapor fluxes ($\leq 5\times10^{-5}$ moles/cm^{2}min). This is, in fact, an advantage in high temperature vaporization studies.

In vaporization kinetics studies the weight loss of the sample may be measured as a function of time. Microbalance techniques[22] allow one to detect weight changes continuously in vacuum in the range of 10^{-8}-10^{-5} g. Torsion balances may be used to an even higher degree of sensitivity. Mass spectrometric monitoring of the vapor composition allows the detection of ~10^5 particles/sec which corresponds to a weight loss of $\approx 10^{-11}$ g/sec.[23] Thus, the use of a mass spectrometer in addition to a microbalance extends the temperature range of the investigation appreciably. The two techniques are complimentary and provide valuable information in studies of the evaporation mechanism. Weight loss measurements by microbalance techniques give absolute evaporation rates while mass spectrometric monitoring of the vaporization reaction allows one to determine the vapor composition and relative changes in the vapor composition from which the evaporation rates may be calculated.

Other techniques such as optical[24] or surface ionization[25] detection of the vaporizing species during the vaporization reactions have also been used successfully to monitor evaporation rates.

HIGH TEMPERATURE VAPORIZATION MECHANISMS

Among the substances most frequently utilized in the high temperature technology, the oxides, nitrides, carbides, silicides and borides of elements occupy a prominent place. Study of the evaporation mechanism of these solids would be of great importance in predicting their performance

under a variety of environmental conditions. Unfortunately, it is difficult, at present, to obtain most of these materials in pure single crystal form. In addition, the experimental problems of carrying out the vaporization studies at very high temperatures make definitive kinetic measurements very difficult to perform.

We can find non-refractory compounds, however, which are likely to show vaporization characteristics almost identical to that of certain groups of refractories. Since these materials vaporize in an easily accessible temperature range, studies of their evaporation mechanism may be used to shed light on the vaporization mechanism of different groups of refractory compounds. We shall discuss studies of the evaporation mechanisms of several non-refractory compounds and summarize the results of recent vacuum vaporization studies of refractories. It is hoped that the extension of these vaporization studies using other solids will allow the determination of the evaporation mechanism of different groups of refractories.

EVAPORATION MECHANISMS LEADING TO CONGRUENT VAPORIZATION

Dissociative Vaporization

There are large groups of substances which maintain a nearly constant solid composition during vaporization into vacuum. Some of these solids dissociate to their atomic constituents or molecular aggregates of their constituents. For diatomic substances of this type the dominant net vaporization reaction can be written as

$$AB(solid) \rightarrow A(vapor) + \frac{1}{y} B_y(vapor) \qquad (4)$$

where y = 1, 2, or 4 in most cases. Thus, the condition of congruent vaporization may be expressed as $\frac{dA(vapor)}{dt} = y\frac{dB_y(vapor)}{dt}$. These materials may exhibit ionic or partly ionic character (NH_4Cl, ZnO, CdS, etc.) or more covalent type bonding (SnO_2, GaN, GaAs). Compounds of the II - VI and III - V groups of elements in the periodic table vaporize in this manner. Most of the compounds which were studied so far show evaporation rates which are appreciably smaller than the maximum rate ($\alpha << 1$). We shall restrict the discussion to those materials whose evaporation kinetics have been studied in some detail to illustrate the types of vaporization mechanisms leading to dissociative congruent vaporization.

In Table 1 we list those solids which vaporize dissociatively and whose evaporation rates have been investigated. The dominant vaporization reaction is given and the experimental conditions (vacuum vaporization or equilibrium) under which it was determined is indicated. The heats of evaporation, ΔH_v^o, (kcal/mole of solid), the activation enthalpies of vaporization, ΔH_v^*, (kcal/mole of solid), and the average evaporation coefficients, $\bar{\alpha}$, for the studied temperature range are listed whenever they have been determined. The temperature range of the experiments and the type of samples (single crystal or polycrystalline) which were used are also indicated.

Charge transfer controlled vaporization of CdS. The vaporization of CdS single crystals has been studied in detail.[2] The compound vaporizes according to the dominant net reaction, CdS(solid) → Cd(vapor) + 1/2 S_2(vapor). Cadmium sulfide is a semiconductor [E_{gap}(300°K) = 2.41 ev] and its electrical conductivity can change by ten orders of magnitude due to the presence of minute excesses of cadmium or sulfur in the lattice (p.p.m. above the steady state composition[10]) or due to the presence of electrically active impurities[11] (in p.p.m. concentrations). The following vaporization studies were carried out.

Temperature dependence of the vacuum evaporation rate. The stable c-face of the hexagonal single crystals[19] was used in these studies (Fig. 1). The activation enthalpy has a value of $\Delta H_v^* = 50.3$ kcal/mole and the heat of sublimation is $\Delta H_v^o = 75.2$ kcal/mole of the vaporizing solid in the temperature range 650-800°C. The evaporation coefficient is $\bar{\alpha} \leq 10^{-1}$ in this range.[6]

The effect of light on the evaporation rate. The charge carrier concentration at the vaporizing surface can be varied by illumination with light of greater than band gap energy.[9,18] The light intensity in these experiments has to be high enough to be able to generate electron-hole pairs in concentrations of the same order of magnitude of, or larger than, the free carrier concentration already available in the dark at the evaporation temperatures. This condition was met for high resistivity CdS crystals. The evaporation rate was found to increase linearly with light intensity in the studied range (Fig. 2).

The vaporization of copper doped CdS. Copper is an electron acceptor in CdS which reduces the free electron concentration of the pure crystal by orders of magnitude. It should be noted that light which affected the evaporation rate of undoped CdS crystals had no effect on the evaporation of copper doped samples. This copper in the CdS crystal lattice either reduces the free carrier lifetime markedly or introduces cadmium vacancies which play an important role in the charge transfer. When the CdS crystal was uniformly saturated with copper at the temperature of evaporation, the evaporation rate of Cu-doped CdS decreased by more than 50% from that of the evaporation rate of the undoped sample[11] (Fig. 3).

In order to investigate the dependence of the evaporation rate on the changing concentration of copper at the crystal surface, copper was vacuum deposited on only the $(000\bar{1})$-face of the undoped crystal. Then, the other c-face (0001) was allowed to vaporize while copper diffused into the sample from the back surface. This way the vaporizing surface retreats while the copper diffusion front moves toward the vaporizing face. When the copper diffusion front reaches the vaporizing surface a rapid change in the copper surface concentration occurs[11] which gives rise to an exponential decrease of the evaporation rate (Fig. 4).

The vaporization of cadmium and sulfur doped CdS. The crystals were doped[10] with excess cadmium or sulfur at elevated temperatures (900° - 1100°C) then were quenched to freeze in the high temperature solubilities. Although the solubilities of excess cadmium or sulfur in CdS are very small ($\leq$ 100 p.p.m.), the electron concentration can be changed by more than ten orders of magnitude by these doping treatments. The initial evaporation rates of both cadmium and sulfur-doped CdS crystals were

lower by almost an order of magnitude than the evaporation rate of the undoped crystals at the same temperature (700°C). The excess cadmium or sulfur, however, diffuses out of the crystal during vaporization. When all of the excesses are removed and the crystal attains its steady state composition,[10,15] the evaporation rate undergoes a sharp transient and returns to the value which is characteristic of the undoped samples (Fig. 5).

Surface concentration dependence of the evaporation rate. The surface concentrations of the vaporizing species, Cd(v) and S_2(vapor) were varied by using an atomic beam of cadmium and/or a molecular beam of sulfur. The molecular beams were allowed to impinge on the vaporizing surface at a given temperature.[6] Care was taken to maintain a sufficiently long mean free path of all vapor species to exclude the possibility of gas phase collisions. The rate of vaporization, J_{CdS}, was measured as a function of the rate of impingement of sulfur (J_{S_2}) or cadmium (J_{Cd}). It was found that the evaporation rate of CdS is proportional to the -1/2 power of the sulfur flux ($J_{CdS} \approx J_{S_2}^{-1/2}$) as shown in Fig. 6, and that the cadmium atomic beam had no appreciable effect on the evaporation rate.

The results of these experiments allow us to deduce the detailed mechanism of CdS vaporization.[2,18] The presence of excesses of cadmium and sulfur and copper in CdS decreased the evaporation rates markedly. These impurities have low solubilities in cadmium sulfide, but they can change the free carrier concentration in the vaporizing crystals by orders of magnitude. It is apparent that the concentration of charge carriers plays an important role in the vaporization process. The effects of electrically active impurities and of light on the evaporation rate

indicate that the vaporization is controlled by a charge transfer process. The vaporization reaction steps which can be deduced from the available experimental information are: a) diffusion of excess cadmium or sulfur to the surface, b) electron transfer to neutralize the cadmium ions at the surface, c) hole transfer to neutralize the sulfur ions at the surface, d) association of sulfur atoms, e) desorption of sulfur molecules, and f) desorption of cadmium atoms. The detailed analysis of the rate controlling steps under the different experimental conditions has been reported elsewhere.[2,18] In brief, under vacuum evaporation conditions for undoped CdS crystals in dark or in light, steps (b) and (c) are indistinguishable and rate limiting. For sulfur and cadmium doped crystals, reaction (a) controls the evaporation rate. For the vaporization of copper doped CdS, step (b) is the possible slow step.

It is interesting to note the self-correcting evaporation process of sulfur and cadmium doped CdS.[10] In the presence of minute excesses of the crystal constituents the evaporation rate was found to decrease markedly (Fig. 1). Thus, the steady state composition has a maximum rate of vaporization and any off-stoichiometry is self-corrected by the out-diffusion of the excess. This composition dependence of the evaporation rate indicates that, although the compound dissociates upon vaporization, the vaporization of the Cd(vapor) and S_2(vapor) are not independent but must be controlled by a single reaction step which takes place at the vaporizing surface. Searcy and Leonard[31] have found that oxygen doped ZnO shows the same self-correcting vaporization characteristics, i.e., excess oxygen decreases the evaporation rate of zinc oxide and must diffuse out of the lattice before the solid can return to its steady state rate

of vaporization. This type of self-correcting composition dependent evaporation rate may well be the property of the majority of congruently vaporizing solids.

It is likely that the charge transfer controlled vaporization mechanism is more generally applicable to a group of congruently vaporizing solids. Binary compounds such as oxides, halides and sulfides of Ag, Pb, Cd and Sn in addition to the IIB - VIA compounds are likely candidates for vaporization by the charge transfer mechanism. The experimental information available at the present, however, does not allow us to propose any general correlation.

Vaporization Characteristics of III-V Compounds

Compounds of the III-V elements also dissociate upon vaporization. The activation enthalpies of vaporization of several solids which belong to this group are given in Table 1. The temperature dependence of the vacuum evaporation rate of GaN(solid) has been studied by Munir and Searcy[27] and the activation enthalpy of vaporization has been determined. Shoemaker[17] has found that in the presence of liquid gallium the evaporation rate of GaN increases by an order of magnitude. Liquid gallium seems to catalyze the evaporation process by possibly dissolving the vaporizing species.[17] The presence of a liquid phase provides an alternate reaction path to the breaking up of the crystal lattice during vaporization. Other examples to the catalysis of vaporization by the presence of a liquid are the evaporation of arsenic or red phosphorus in the presence of molten thallium.[16]

Recent evidence indicates[40] that the evaporation mechanism of some of the III-V compounds may change as a function of temperature. It was found that for gallium arsenide, GaAs, the log J_v vs $1/T^\circ K$ plot does not yield a straight line. The resultant curve breaks sharply at about 850°C and one can assign different activation enthalpy values for the low and high temperature portion of the curve. At elevated temperatures GaAs vaporizes according to the net reaction GaAs(solid) $\rightarrow$ Ga(vapor) + $\frac{x}{2}$ As_2(vapor) + $\left(\frac{1-x}{4}\right)$ As_4(vapor). The detailed mechanism of evaporation is being studied at the present in our laboratory. It is likely that the change of the evaporation mechanism may be due to the presence of a liquid gallium phase in a given temperature range.

Boron nitride, BN(solid), on the other hand shows non-congruent vaporization.[41] Boron(solid) condenses out on the vaporizing surface and further vaporization is limited by the out-diffusion of nitrogen through the boron layer. Thus, the IIIA-VA compounds seem to show a transition from congruent to non-congruent vaporization. Which of the compounds belongs to one group or to the other seems to depend on the relative evaporation rates of the IIIA and VA compound constituents. If the IIIA group component is liquid at the vaporization temperature, the evaporation rate may be increased by the presence of the excess IIIA metal. If the IIIA component remains solid at the vaporization temperature the evaporation rate may become limited by the out-diffusion of the VA constituent through a layer of the solid IIIA constituent which has condensed out at the vaporizing surface.

These results indicate that the vaporization of the IIIA and Va components from the surface of the III-V compounds follow independent

reaction paths. They seem to have different evaporation mechanisms which should give rise to different evaporation coefficients for the two components.

Future studies using single crystal GaAs and other III-V compounds will be aimed at the understanding of the detailed vaporization reactions of both the IIIA and the VA components.

Congruently Vaporizing Nitrides

Several nitrides show congruent dissociative vaporization at well-defined solid compositions under conditions of vacuum vaporization. All of these compounds have vacuum evaporation rates which are more than two orders of magnitude smaller than the maximum evaporation rates in the studied temperature range. Both II-V compounds, Be_3N_2 and Mg_3N_2 belong to this group and they both show vacuum evaporation rates which are about three orders of magnitude smaller than the maximum rates in the studied temperature ranges.[26,28] Among the III-V nitrides, AlN[26,41] and GaN,[27] vaporize congruently. Among the nitrides of the transition elements only $TiN_{0.8}$ seems to belong to this group.[29] Some of the vaporization characteristics of these compounds are given in Table 1.

Congruently Vaporizing Oxides

The majority of the oxides vaporize congruently, frequently with the formation of several oxide vapor molecules of the general formula $M_xO_y(vapor)$ $(x = 1,2,\ldots\ y = 1,2,\ldots)$. Several of these compounds were studied under vacuum evaporation conditions. In all of these studies, however, only the temperature dependence of the vaporization rate was monitored to obtain the activation enthalpy of vaporization.

Therefore, the vaporization mechanism of these compounds cannot be deduced at the present.

The vaporization of tin oxide, SnO_2, was studied by Searci and Hoenig.[42] They report vacuum evaporation rates which are roughly an order of magnitude lower than the maximum rate as predicted by Eq. (2). The vaporization of Al_2O_3, Ga_2O_3, and In_2O_3 was studied by Burns et al.[14,31] Again the vacuum vaporization rates are markedly smaller than the maximum rates. They have also observed a discontinuity in the evaporation rate at the melting point where the rates show a sudden three-fold increase. Thus, it is apparent that the vaporization is controlled by the breaking away of the vaporizing units from the crystal lattice at the vaporizing surface. Once the crystal lattice collapses vaporization is accelerated and becomes limited by the desorption rate of the vaporizing species.

Several refractory oxides vaporize by the sublimation of the metal atom in addition to the oxide and the oxygen vapor molecules.[43] For example, the vapor composition over thorium oxide shows a ratio, $ThO/Th \approx 4$ under certain experimental conditions.[44] CaO and MgO break up completely[45] according to the reaction $MO(solid) \rightarrow M(vapor) + 1/2\ O_2(vapor)$. Other congruently vaporizing oxides form more than one type of oxide vapor species[45] (vanadium and tungsten oxides and titanium dioxide). The vaporization of boron and barium oxides on the other hand[45,46] seem to yield BaO and B_2O_3 vapor molecules.

Associative Vaporization

There is a large group of solids which associate upon vaporization. It is well known[47,48] that the alkali halides vaporize according to the

dominant reaction*

$$AB(solid) \rightarrow xAB(vapor) + \frac{(1-x)}{2} (AB)_2(vapor) \qquad (5)$$

The evaporation mechanism of sodium chloride single crystals is under investigation at the present. Among the monatomic solids which vaporize in this manner, the vaporization of graphite,[49,50] arsenic and phosphorus[16] have been studied to some extent.

In Table 2 we list those congruently vaporizing solids which associated upon vaporization. The dominant vaporization reactions are given together with the heats of vaporization, ΔH_v^o, (kcal/mole of solid) and the activation enthalpies of vaporization, ΔH_v^*, (kcal/mole of solid). The average evaporation coefficients, $\bar{\alpha}$, for the studied temperature ranges are also listed wherever they have been determined.

Evaporation Mechanism of NaCl Single Crystals

Temperature dependence of the vacuum evaporation rate. The (100)-face of NaCl single crystals was used in most of these experiments. This face cleaves easily and is stable under conditions of vacuum vaporization. The temperature dependence of the evaporation rates were measured using a microbalance and also by using a mass spectrometer in the temperature range 400 - 650°C. The dimer concentration is roughly 12% of the total vapor concentration in this temperature range. It was found that the activation enthalpies of vaporization which were obtained using different NaCl crystal batches varied by as much as 10 kcal. (The crystals were of optical grade obtained from Harshaw Chemical Company.)

* In some cases (LiF for example) the existence of higher polymers has been well established.[47]

Representative curves of our results and that of Kusch, et al.[47,48] and the maximum rate of vaporization as determined by effusion studies[56] are shown in Fig. 7. We also list in Table 3 representative values of the activation enthalpies of vaporization which were obtained for both the monomer and the dimer vapor species.

The vaporization rate of doped NaCl single crystals. Since the crystals used in our studies were of the highest available purity it was thought that the presence of minute uncontrolled impurities were actually responsible for the varying evaporation rates. Therefore, crystals were doped with a variety of impurities and defects; OH^-, Ca^{2+}, O_2^-, Br^-, Na and Cl (excesses) to verify their effect on the vacuum evaporation rate. The presence of sodium ion vacancies or chloride ion vacancies which were introduced by heating the crystals in sodium or chlorine vapor had no effect on the vaporization rate. Unlike the lattice defects of the IIB-VIA compounds (CdS, ZnO) these vacancies seem to diffuse rapidly from the NaCl crystal lattice at the evaporation temperatures. Thus, except for a short transient period when the crystal is first heated, the crystal retains congruency throughout the vaporization. It was also found that impurity ions which fit into the anion or cation sites in NaCl without introducing any marked distortion of the crystal lattice had also no effect on the vaporization rate. These were Ca^{2+}, in concentrations as much as 0.5 mole %, and OH^- ions in an unknown concentration sufficient to produce a distinct absorption peak in the infrared spectrum at 2.76μ.

When oxygen (O_2^-) ions were introduced into the NaCl lattice, however, the evaporation rates have changed with respect to the undoped crystals. Upon introduction of oxygen the rate increased and the activation enthalpies of vaporization of both monomers and dimers decreased by several kilocalories. Also, the dimer to monomer ratio decreased by about 40% in the temperature range studied.

These studies are still in progress using sodium chloride crystals which are grown by pulling from the melt. The starting material had been zone refined under an HCl atmosphere in order to remove bromine and oxygen containing impurities. Also, crystals have been produced with a high dislocation content in order to study the effect of dislocation density on the evaporation mechanism. These effects will be discussed.

The Vaporization of Graphite

The temperature dependence of the graphite vaporization rate into vacuum was measured by several investigators. Recently Burns et al.[49] have reported on a mass-spectrometric study of free vaporization of graphite using single crystals of well-defined orientation. Comparison of this data with equilibrium vapor pressure determinations[50] indicates that the vacuum evaporation rates of all carbon vapor species are approximately an order of magnitude smaller than the maximum rates at 2500°K. It is apparent from the experimental results that at higher temperatures C_3 molecules are the most abundant vapor species.

Vaporization of Arsenic and Phosphorus

The vaporization of arsenic, red and white phosphorus into vacuum has been investigated by Brewer and Kane[16] using polycrystalline samples. More recently Rosenblatt[57] has measured the evaporation rates of single crystal arsenic.

The dominant vapor species over solid arsenic is As_4(vapor). The vaporization rate into vacuum was found to be seven orders of magnitude smaller than the maximum rate as determined by equilibrium studies. The (111) crystal face gave lower evaporation rates than that of the (110)-face. From the temperature dependence of the evaporation rate the activation enthalpy has been determined and is given in Table 2.

The evaporation rates of two modifications of phosphorus, red and white have been investigated. Red phosphorus has a crystal structure with equal energies for all P-P bonds while white phosphorus is a molecular crystal which contains P_4 units with only Van der Waals forces[16] between the P_4 molecules. The dominant vapor species over both forms of phosphorus are P_4 molecules. White phosphorus does not undergo much rearrangement upon vaporization and exhibits vaporization rates equal to the maximum rates predicted by Eq. (2). Red phosphorus, however, shows evaporation rates which, in the same temperature range, 275-400°C, are six orders of magnitude smaller than the maximum rate as determined by equilibrium studies. The activation enthalpies of vaporization for both modifications are given in Table 2.

Non-Congruent Vaporization

Compounds which belong to this group of solids have constituents with markedly different evaporation rates. For a diatomic solid, AB,

of this type, the criteria of non-congruent vaporization may be written as $\frac{dA(vapor)}{dt} \neq \frac{dB(vapor)}{dt}$. Thus, the solid composition may change markedly during vaporization. This kind of vaporization process indicates that the vaporization of the compound constituents must be independent and follow separate reaction paths. Although a large fraction of the refractory compounds vaporize in this manner (most carbides, borides, and silicides), the detailed vaporization mechanisms which lead to non-congruent vaporization have not been investigated extensively. It is possible however, to describe several types of vaporization processes which could lead to the non-congruent evaporation of solids.

Diffusion Controlled Vaporization

One type of net vaporization reaction which leads to diffusion controlled vaporization may be written as

$$AB(solid) \rightarrow A(solid) + B(vapor) \qquad (6)$$

The kinetics of this type of vaproization reaction may be divided into two stages: a) transient vaporization and b) steady state vaporization.

a) At the onset of the evaporation the compound decomposes rapidly at the vaporizing surface. One of the constituents, (B(vapor)), is removed to the vapor phase while the other constituent, A(solid), condenses at the interface. Once the whole surface of AB(solid) is covered with A(solid) the vaporization rate will depend on the rate of arrival of component B to the vaporizing surface via diffusion through A(solid). Initially there is only a thin layer of A(solid) covering the compound surface through which diffusion of B(solid) may be fairly rapid. Thus,

the interface between AB(solid) and A(solid) moves deeper into the solid while the vaporizing surface remains virtually stationary. As the A(solid) layer thickens, the rate of arrival of B(solid) from the AB(solid) - A(solid) interface to the vaporizing surface diminishes. Since the evaporation rate depends on the surface concentration of B(solid), it also decreases rapidly.

The extent of this transient evaporation rate which is controlled by the diffusion of B(solid) through an increasingly thicker layer of A(solid) depends on the temperature, the porosity of the condensing layer of A(solid) and the diffusion rate of B through A(solid). The kinetics of such a transient vaporization process can be even more complicated if a phase transformation occurs during the continuous change of the solid composition.

Nevertheless, the mechanism of diffusion which controls the vaporization of B(solid) and thus the decomposition rate may be deduced from the transient vaporization rate. For example, if we assume that the rate of vaporization of AB(solid) is a function of the concentration of B(solid) at the vaporizing surface, and that this concentration is already very small[10] the concentration of B(solid), C_B, at any point in A(solid) is given by[10]

$$C_B = \sum_{\ell,m,n} A_{\ell,m,n} \exp(-\alpha_{\ell,m,n} t) \qquad (7)$$

where

$$\alpha_{\ell,m,n} = D\pi^2 \left[\frac{(2\ell+1)^2}{a^2} + \frac{(2m+1)^2}{b^2} + \frac{(2n-1)^2}{c^2} \right] \qquad (8)$$

where D is the diffusion constant and a, b, and c are the lengths of the edges of the crystal. For large times only the first term in the sum need be considered ($\ell = m = n = 0$) so we have

$$C_B \cong \exp(-D^2)\left(\frac{1}{a^2} + \frac{1}{b^2} + \frac{1}{c^2}\right) t \qquad (9)$$

Since the evaporation rate is given by $-\frac{dB(solid)}{dt} = k\, C_B$ from the time dependence of the evaporation rate the diffusion constant can be calculated. It is apparent, however, that the mechanism of diffusion controlled vaporization can be different from system to system. The boundary conditions used to solve the diffusion equation should be modified so that the resulting solution gives a good fit to the experimental transient vaporization rate data.[58]

b) The increasing thickness of the condensed layer A(solid) finally reduces the diffusion rate of B(solid) to the vaporizing surface to such a small value that its evaporation rate approaches the evaporation rate of A(solid) $\left[\left.\frac{dB(vapor)}{dt}\right|_{A(solid)} \approx \frac{dA(vapor)}{dt}\right]$. When this happens A(solid) is removed at the vaporizing surface as rapidly as it is condensed at the AB(solid) - A(solid) interface. Thus, the A(solid) layer has reached its limiting thickness and steady state vaporization of AB(solid) commences. The limiting thickness of A(solid) at the vaporizing surface may be very small (for example if the diffusion rate of B in A(solid) is slow) or may be infinite (the whole compound, AB(solid) decomposes before steady state vaporization can be attained). Under these steady state diffusion conditions however, even non-congruently vaporizing solids will show an apparent congruent vaporization rate.

Another type of vaporization reaction which leads to non-congruent evaporation may be written as

$$AB(solid) \rightarrow A(melt) + B(vapor) \qquad (10)$$

After the rapid removal of B(solid) from the vicinity of the vaporizing surface further vaporization may be limited by the diffusion of B(solid) through the melt. This process is expected to be more rapid than the solid state diffusion process discussed previously. It is likely that non-congruently vaporizing solids of this type can vaporize with nearly maximum rate. The liquid phase is unlikely to provide the solid with a protective coating as a condensing solid phase frequently does.

ACKNOWLEDGMENT

This work was performed under the auspices of the United States Atomic Energy Commission.

References

1. Lewis, G. N. and M. Randall, Thermodynamics, revised by K. S. Pitzer and L. Brewer, McGraw-Hill, New York, 1961.
2. Somorjai, G. A. and J. E. Lester, Prog. in Solid State Chem., 4 (1967).
3. Hirth, J. P. and G. M. Pound, Condensation and Evaporation, Pergamon Press, New York, 1963.
4. Knacke, O. and I. N. Stranski, Progr. Metal Phys., 6, 181 (1956).
5. Somorjai, G. A., Condensation and Evaporation of Solids, E. Rutner, P. Goldfinger and J. P. Hirth, Eds., Gordon and Breach Science Publishers, New York, 1964.
6. Somorjai, G. A., and D. W. Jepsen, J. Chem. Phys., 41, 1389 (1964).
7. Burton, W. K., N. Cabrera, and F. C. Frank, Phil. Trans. Roy. Soc. (London) A243, 299 (1951).
8. Winterbottom, W. L. and J. P. Hirth, Condensation and Evaporation of Solids, E. Rutner, P. Goldfinger and J. P. Hirth, Eds., Gordon and Breach Science Publishers, New York, 1964.
9. Somorjai, G. A., Surface Sci., 2, 298 (1964).
10. Somorjai, G. A. and D. W. Jepsen, J. Chem. Phys., 41, 1394 (1964).
11. Somorjai, G. A. and H. B. Lyon, J. Chem. Phys., 43, 1456 (1965).
12. Hirschwald, W., F. Stolze, and I. N. Stranski, Z. Physik Chem. Neue Folge, 42, 96 (1964).
13. Jepsen, D. W. and G. A. Somorjai, J. Chem. Phys., 39, 1665 (1963).
14. Burns, R. P., Ph.D. Dissertation, University of Chicago, (1965).
15. Somorjai, G. A. and J. E. Lester, J. Chem. Phys., 42, 4140 (1965).
16. Brewer, L. and J. S. Kane, J. Phys. Chem. 59, 105 (1955).

17. Schoonmaker, R. C., A. Buhl, and J. Lemley, J. Phys. Chem. 69, 3455 (1965).

18. Somorjai, G. A. and J. E. Lester, J. Chem. Phys., 43, 1450 (1965).

19. Somorjai, G. A. and N. R. Stemple, J. Appl. Phys., 35, 3398 (1953).

20. Rosenblatt, G. M., J. Electrochem. Soc. 110, 563 (1963).

21. Littlewood, R. and E. Rideal, Trans. Faraday Soc., 52, 1598 (1956).

22. Vacuum Microbalance Techniques, Vols. 3 and 4, Plenum Press, New York, 1963, 1965.

23. McDowell, C. A., Mass Spectrometry, McGraw-Hill, New York, 1963.

24. Brebrick, R. F. and A. J. Strauss, J. Chem. Phys. 41, 197 (1964).

25. Kusch, P., J. Chem. Phys. 28, 1075 (1958).

26. Blank, B., Ph.D. Dissertation, University of California, Berkeley, UCRL-16018, June 1965.

27. Munir, Z. A. and A. W. Searcy, J. Chem. Phys. 42, 4223 (1965).

28. Hoenig, C. L., Ph.D. Dissertation, University of California, Berkeley, UCRL-7521, 1954.

29. McClaine, L. A., C. P. Coppel, Technical Report AFML-TR-65-299 (1965).

30. Leitnaker, J. M., AEC Technical Report LA-2402 (1960).

31. Leonard, R. B., M.S. Thesis, University of California, Berkeley, UCRL-17108, December 1966.

32. Neuhaus, A. and W. Retting, Z. Electrochemie 62, 33 (1958).

33. Jeunehomme, M., Ph.D. Dissertation, University Libre de Bruxelles, Belgium (1962).

34. Wosten, W. J., J. Phys. Chem. 65, 1949 (1961).

35. Gregory, N. W., J. Phys. Chem. 67, 618 (1963).

36. Motzfeldt, K., J. Phys. Chem. 59, 139 (1955).

37. Chaiken, R. F., D. J. Sibett, J. E. Sutherland, D. K. Van de Mark, and A. Wheeler, J. Chem. Phys., 37, 3211 (1962).

38. Spingler, H., Z. Physik. Chem. (Frankfurt), B52, 90 (1942).

39. Schultz, R. D. and A. O. Dekker, J. Phys. Chem., 60, 1095 (1956).

40. Miller, D. P., J. G. Harper, and T. R. Perry, J. Electrochem. Soc., 108, 1123 (1961).

41. Hildenbrand, D. L. and W. F. Hall, J. Phys. Chem. 67, 888 (1963).

42. Hoenig, C. L. and A. W. Searcy, J. Am. Ceram. Soc. 49, 128 (1966).

43. Panish, M. B., J. Chem. Phys., 34, 2197 (1961).

44. Ackerman, R. J., E. G. Rauh, R. J. Thorn, and M. C. Cannon, J. Phys. Chem., 67, 762 (1963).

45. Drowart, J., Condensation and Evaporation of Solids, E. Rutner, P. Goldfinger and J. P. Hirth, Eds., Gordon and Breach Science Publishers, New York, 1964.

46. Soulen, J. R., P. Sthapitenowda and J. L. Margrave, J. Phys. Chem., 59, 132 (1955).

47. Kusch, P., Condensation and Evaporation of Solids, E. Rutner, P. Goldfinger and J. P. Hirth, Eds., Gordon and Breach Science Publishers, New York, 1964.

48. Rothberg, G. M., M. Eisenstadt and P. Kusch, J. Chem. Phys., 30, 517 (1959).

49. Burns, R. P., A. J. Jason, and M. G. Inghram, J. Chem. Phys., 32, 1366 (1960).

50. Thorn, R. J. and G. H. Winslow, J. Chem. Phys., 26, 186 (1957).

51. Kane, J. S., Ph.D. Dissertation, University of California, Berkeley, 1955.

52. Eisenstadt, M., G. M. Rothberg, and P. Kusch, J. Chem. Phys., 29, 797 (1958).

53. Hirschwald, W., and I. N. Stranski, Condensation and Evaporation of Solids, E. Rutner, P. Goldfinger, and J. P. Hirth, Eds., Gordon and Breach Science Publishers, New York, 1964.

54. Karutz, I. and I. N. Stranski, Z. Anorg. Allg. Chemie, 292, 330 (1957).

55. Zimm, B. and J. Mayer, J. Chem. Phys., 12, 362 (1944).

56. Becker, K. A., H. J. Forth and I. N. Stranski, Z. Electrochem., 64 373 (1960).

57. Rosenblatt, G. M., Pang-Kai Lee, and M. B. Dowell, 45, 3454 (1966).

58. Somorjai, G. A., Trans. ASM, 57, 26 (1964).

Figure Captions

Fig. 1 Rate of evaporation of CdS single crystal c-face as a function of reciprocal temperature.

Fig. 2 Light intensity dependence of the evaporation rate of sulfur-doped (1200°C, 20 atm) CdS single crystal c-face at 696°C. 100% = 2.0×10^5 $\mu W/cm^2$.

Fig. 3 Evaporation rate of the (0001)-face of CdS at 700°C. The crystal was copper doped at 700°C. Dotted line shows the evaporation rate of undoped crystal.

Fig. 4 Evaporation rate of the (0001)-face of CdS at 729°C while copper diffused into the crystal from the $(000\bar{1})$ face.

Fig. 5 The evaporation rates of CdS single crystal c-faces as a function of time at T = 715°C after cadmium-doping at different temperatures.

Fig. 6 The evaporation rate of CdS single crystal c-face as a function of sulfur impingement rate at 715°C.

Fig. 7 Vaporization rates of the (100) face of several sodium chloride single crystals.

Table 1. The evaporation characteristics of dissociating solids. The heats of evaporation, $\Delta H^{o}_{v(298)}$, the activation enthalpies of vaporization, ΔH^{*}_{v}, and the average evaporation coefficients, $\bar{\alpha}$, are listed wherever they have been determined. The temperature range of the experiments and the type of samples which were used are also indicated.

Compound	Reaction	$\Delta H^{o}_{v(298)}$ [a] (kcal/mole solid)	ΔH^{*}_{v} [b] (kcal/mole solid)	$\bar{\alpha}_{v}$ [b]	Sample	Temp. Range (°K)	Ref.
AlN	$AlN(s) \rightarrow Al(v)+\frac{1}{2}N_2(v)$(in equil)	153	102	5×10^{-3}	polycrystalline	1450-1750	26
GaN	$GaN(s) \rightarrow Ga(\ell)+\frac{1}{2}N_2(v)$(in equil)	23.4	-	3×10^{-3}	"	1200-1400	27
	$GaN(s) \rightarrow Ga(v)+\frac{1}{2}N_2(v)$(in vacuum)	-	83	3×10^{-3}	"	1150-1275	17
Be_3N_2	$Be_3N_2(s) \rightarrow 3Be(v)+N_2(v)$(in equil)	376±3	108±3	5×10^{-3}	"	1600-1870	28
Mg_3N_2	$Mg_3N_2(s) \rightarrow 3Mg(v)+N_2(v)$(in equil)	244	55	10^{-3}	"	1000-1250	26
$TiN_{0.8}$	$TiN_{0.8} \rightarrow Ti(v)+\frac{1}{2}0.8N_2(v)$(in vacuum)	127	-	10^{-3}-10^{-2}	"	1800-2200	29
$ZrB_{1.906}$	$ZrB_{1.906} \rightarrow Zr(v)+1.906B(v)$(in equil)	303	-	2.5×10^{-2}	"	2150-2475	30
Al_2O_3	$Al_2O_3(s) \rightarrow 2Al(v)+3/2\ O_2(v)$(in vacuum)	549	-	3×10^{-1}	"	2100-2500	14,31
Ga_2O_3	$Ga_2O_3(s) \rightarrow Ga_2O(v)+O_2(v)$(in vacuum)	242	-	3×10^{-1}	"	1250-2100	31
In_2O_3	$In_2O_3(s) \rightarrow In_2O(v)+O_2(v)$(in vacuum)	220	-	3×10^{-1}	"	1200-1450	31
SnO_2	$SnO_2(s) \rightarrow SnO(v)+\frac{1}{2}O_2(v)$(in equil)	143±1	90±4	8×10^{-2}	"	1240-1480	28
ZnO	$ZnO(s) \rightarrow Zn(v)+\frac{1}{2}O_2(v)$(in equil)	114.8±1	85±8	2×10^{-3}	single crystal	1300-1530	28,31
CdS	$CdS(s) \rightarrow Cd(v)+\frac{1}{2}S_2(v)$(in vacuum)	81.8±2	50.3±1	10^{-1}	"	870-1170	5,32,33
CdSe	$CdSe(s) \rightarrow Cd(v)+\frac{1}{2}Se_2(v)$(in equil)	79.5±2	55.9±1	10^{-1}	"	870-1150	5,34
$FeCl_3$	$FeCl_3(s) \rightarrow FeCl_2(v)+\frac{1}{2}Cl_2(v)$(in equil)	13.0	(13.0)[c]	10^{-6}	polycrystalline	575-675	35
Na_2CO_3	$Na_2CO_3(s) \rightarrow 2Na(v)+CO_2(v)+\frac{1}{2}O_2(v)$(in equil)	228	-	10^{-2}	"	1200-1380	36
NH_4F	$NH_4F(s) \rightarrow NH_3(v)+HF(v)$(in equil)	36.1	12.2	-	"	373-873	37
NH_4Cl	$NH_4Cl(s) \rightarrow NH_3(v)+HCl(v)$(in equil)	42.3	13.5	10^{-4}	"	390-490	37,38,39
NH_4Br	$NH_4Br(s) \rightarrow NH_3(v)+HBr(v)$(in equil)	44.9	15.0	-	"	373-873	39
NH_4I	$NH_4I(s) \rightarrow NH_3(v)+HI(v)$(in equil)	43.5	16.6	-	"	373-873	39

[a] At 298°K in kcal/mole solid unless otherwise noted.

[b] At avg. T of experiment.

[c] Estimated value.[35]

XBL 676-4114

Table 2

The evaporation characteristics of associating solids. The heats of evaporation, $\Delta H^{o}_{v(298)}$, the activation enthalpies of vaporization, ΔH^{*}_{v}, and the average evaporation coefficients, $\bar{\alpha}$, are listed wherever they have been determined. The temperature range of the experiments and the type of samples which were used, are also indicated.

Compound	Reaction	$\Delta H^{o}_{v(298)}$ [a] (kcal/mole vapor)	ΔH^{*}_{v} [b] (kcal/mole vapor)	$\bar{\alpha}_{v}$ [b]	Temp. Range(°K)	Sample	Reference
NaCl	$NaCl(s) \rightarrow NaCl(v)$(in vacuum)	53.5±1(900°K)	61.7	2×10^{-1}	875-935	single crystal	46,52
	$2NaCl(s) \rightarrow Na_2Cl_2(v)$(in vacuum)	57.4±1(900°K)	67.2	10^{-1}	875-935	"	47,48
LiF	$LiF(s) \rightarrow LiF(v)$(in vacuum)	62.4	--	5×10^{-1}	980-1070	"	25,48
	$2LiF(s) \rightarrow Li_2F_2(v)$(in vacuum)	65.3	--	6×10^{-1}	980-1070	"	25,47,48
	$3LiF(s) \rightarrow Li_3F_3(v)$(in vacuum)	74.9	--	5×10^{-1}	980-1070	"	25,48
Graphite	$C(s) \rightarrow C(v)$(in vacuum)	171	--	2×10^{-1}	2500	"	49,50
	$2C(s) \rightarrow C_2(v)$(in vacuum)	195	--	3×10^{-1}	2500	"	49,50
	$3C(s) \rightarrow C_3(v)$(in vacuum)	187	--	4×10^{-2}	2500	"	49,50
P(red)	$4P(s) \rightarrow P_4(v)$(in vacuum)	28	52	10^{-6}	560-670	polycrystalline	16,51
P(white)	$P_4(s) \rightarrow P_4(v)$(in vacuum)	28	28	1	560-670	"	16,51
As	$4As(s) \rightarrow As_4(v)$(in vacuum)	33	44±2	10^{-7}	545-675	single crystal	16,51
As_2O_3 (claudetitite)	$As_2O_3 \rightarrow xAs_2O_3(v) +$ $(1-x)/2\ As_4O_6(v)$(in vacuum)	22.3[d]	55.5[d]	10^{-6}	373-573	polycrystalline	54,55
As_4O_6 (arsenolith)	$As_4O_6(s) \rightarrow As_4O_6(v)$(in vacuum)	22.3[d]	23.0[d]	1	300-370	"	53,54
$FeCl_3$	$2FeCl_3(s) \rightarrow Fe_2Cl_6(v)$(in equil)	32.6	(38.9)[c]	7×10^{-3}	575-675	"	35

a. At 298°K in kcal/mole of vapor unless otherwise noted.

b. At average temperature of evaporation.

c. Estimated value.[35]

d. Average values in kcal/mole of solid.

XBL 676-4113

Table 3

Representative values of activation energies of vaporization for several NaCl single crystals.

Experiment	$\Delta H^*_{monomer}$ (kcal/mole)	ΔH^*_{dimer} (kcal/mole)
Crystal 1 (100) face	46.5 ± 2	53.5 ± 2
Crystal 2 (100) face	54.0 ± 2	63.0 ± 2
R.E.K.[48] (100) face	61.7 ± 4.6	67.2 ± 4.6
Equilibrium[55]	ΔH°_v = 53.5 ± 1	ΔH°_v = 57.4 ± 2

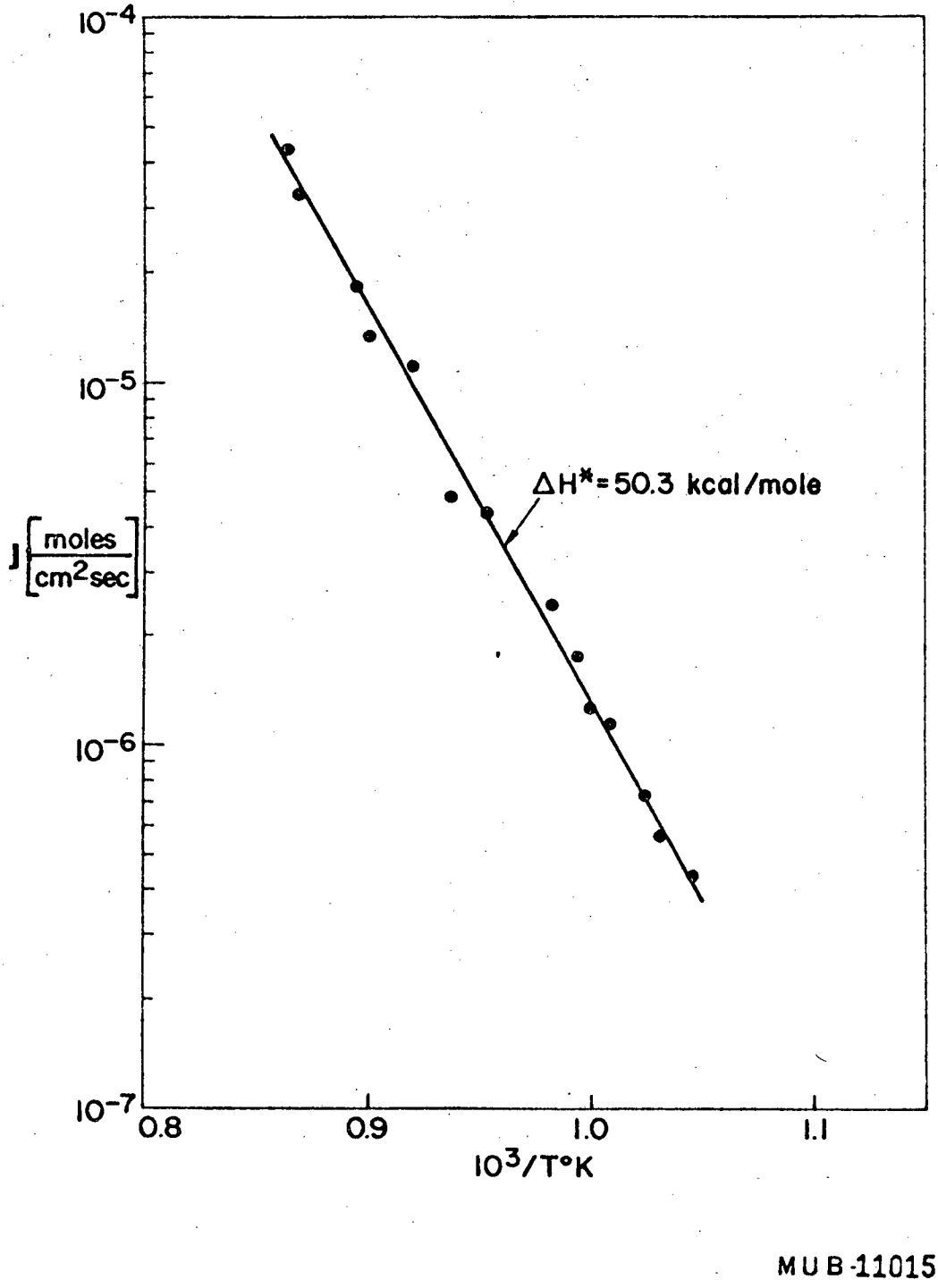
10^{-4}
10^{-5}
10^{-6}
10^{-7}
$J\left[\frac{\text{moles}}{\text{cm}^2\text{sec}}\right]$
$\Delta H^* = 50.3$ kcal/mole
0.8
0.9
1.0
1.1
$10^3/T°K$
MUB-11015

Fig. 1

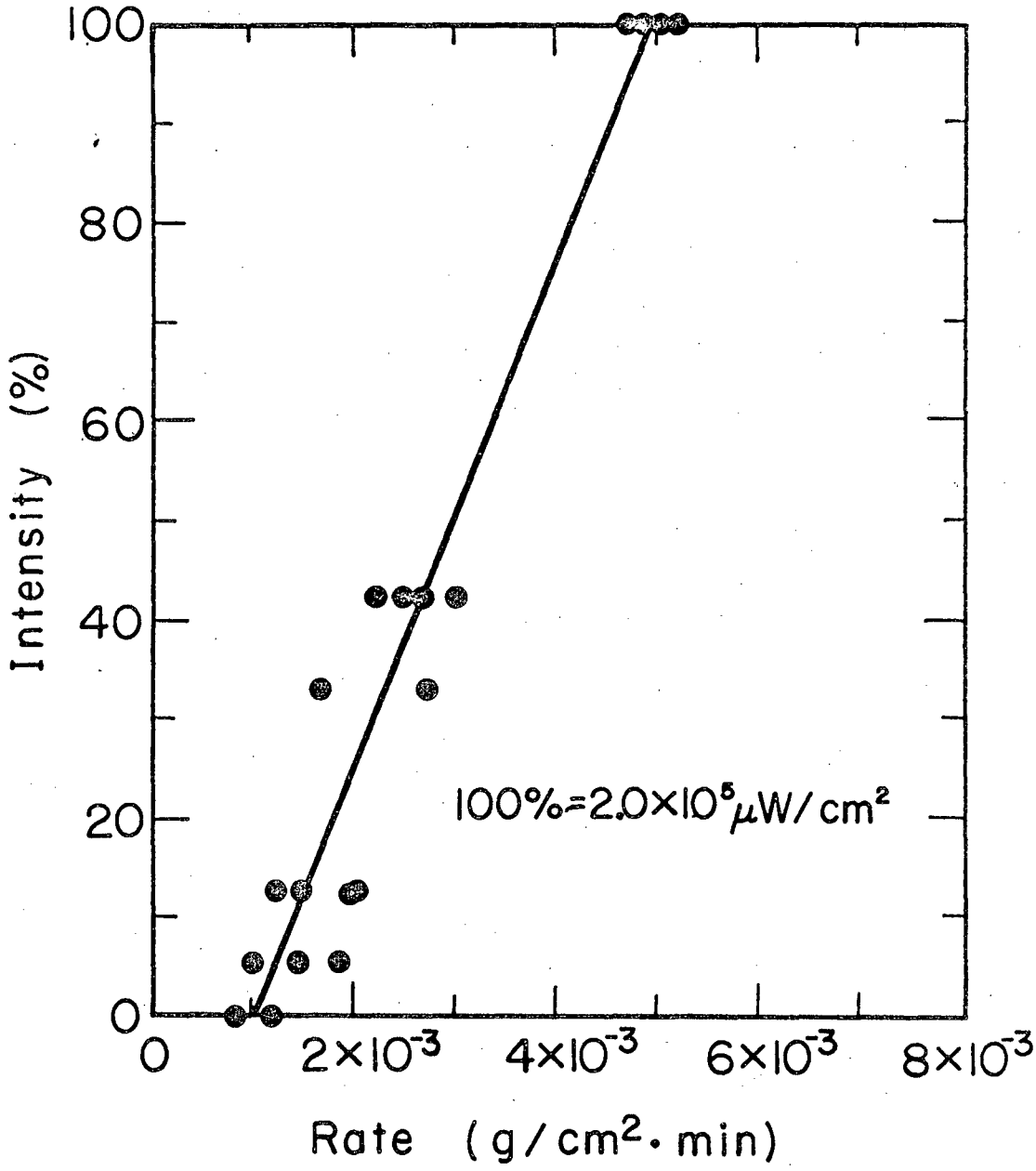

MUB-11118

Fig. 2

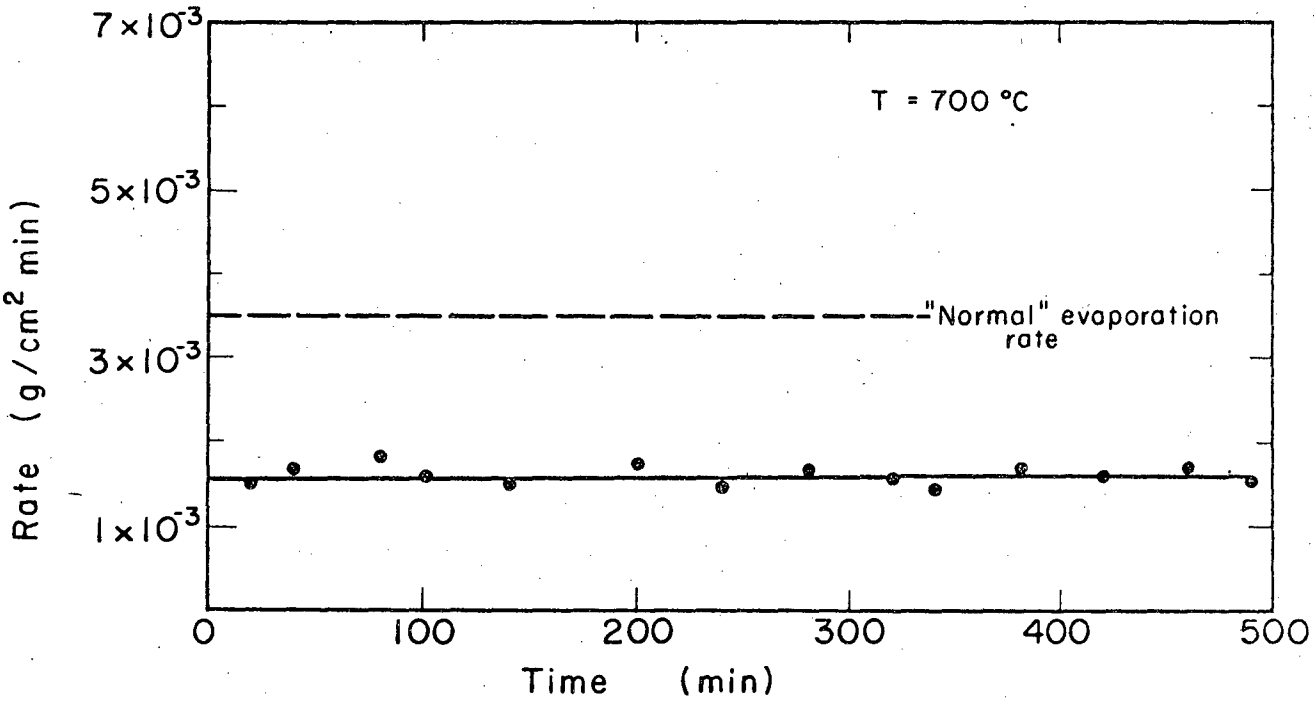
7×10⁻³
5×10⁻³
3×10⁻³
1×10⁻³
Rate (g/cm² min)
T = 700 °C
"Normal" evaporation rate
0
100
200
300
400
500
Time (min)
MUB-5954

Fig. 3

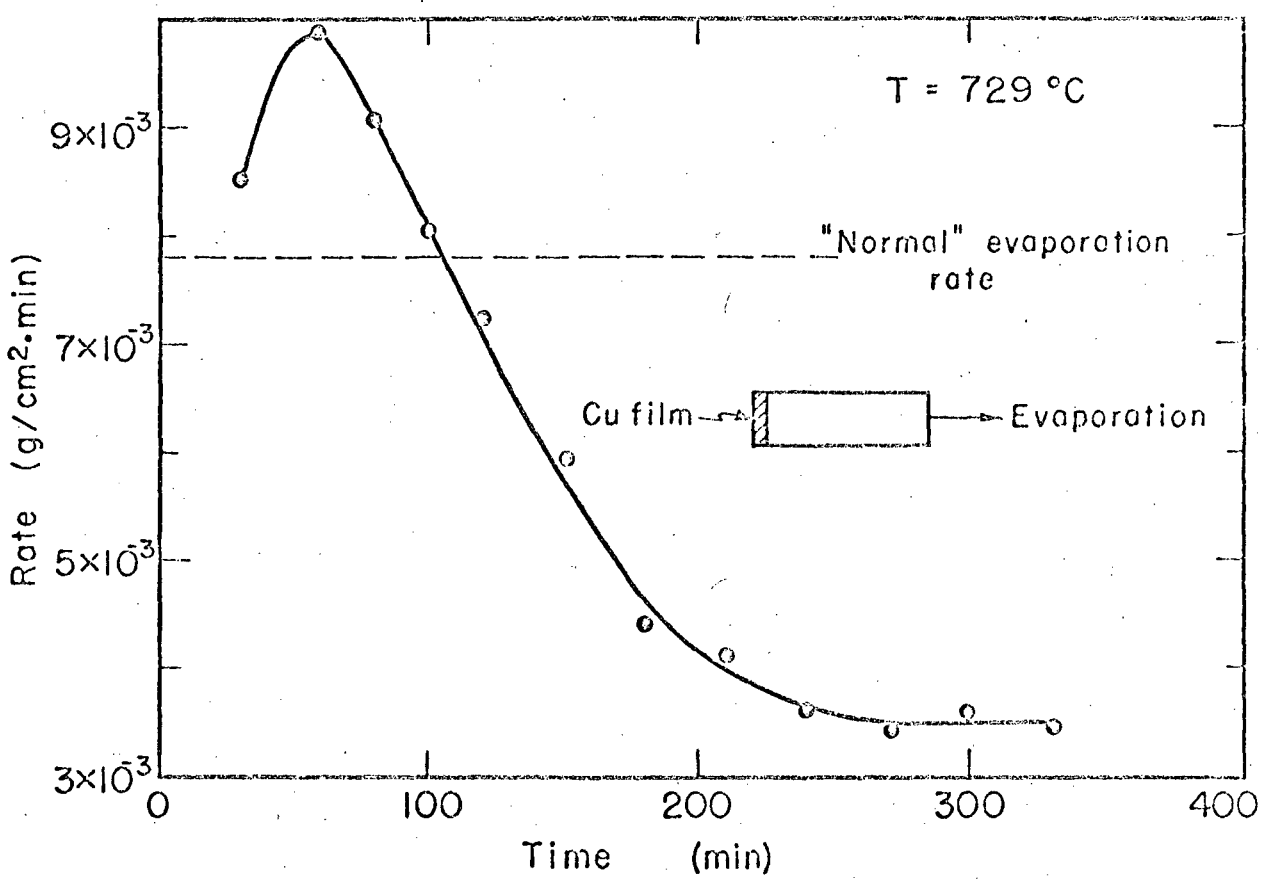
T = 729 °C
"Normal" evaporation rate
Cu film
Evaporation
Rate (g/cm².min)
9×10⁻³
7×10⁻³
5×10⁻³
3×10⁻³
0
100
200
300
400
Time (min)
MUB-5957

Fig. 4

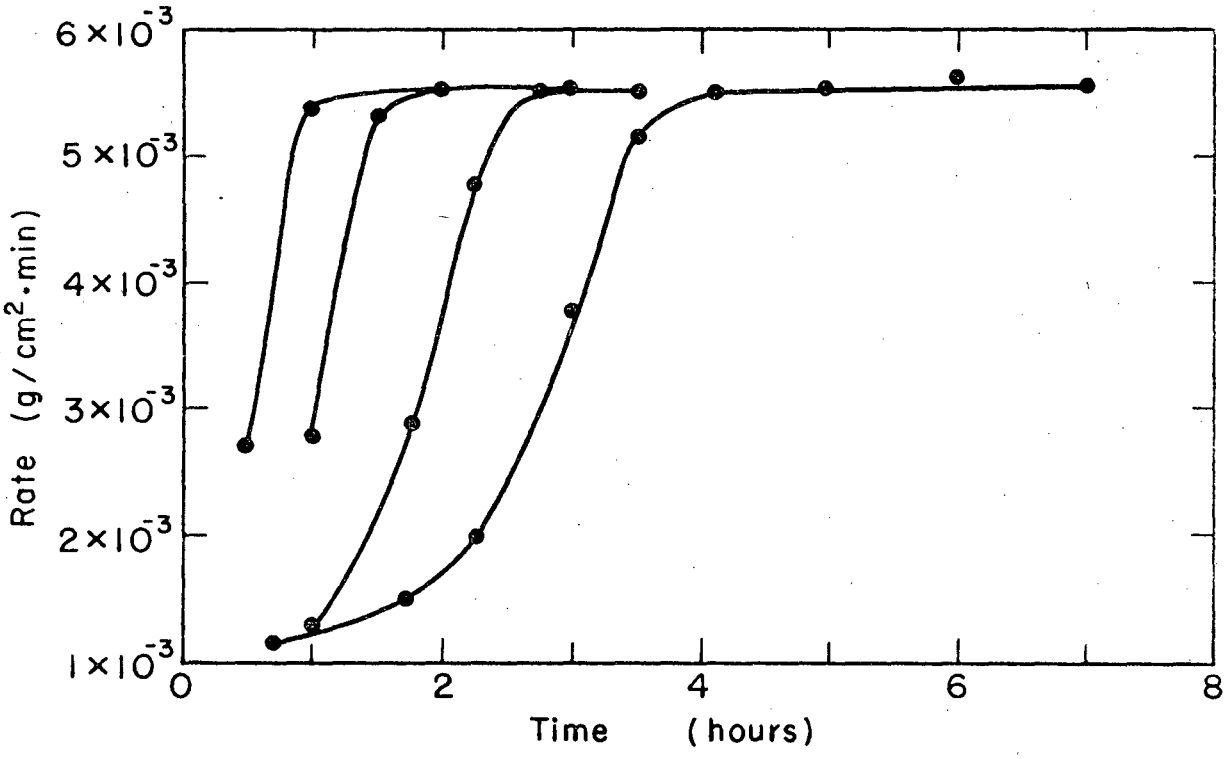
6×10⁻³
5×10⁻³
4×10⁻³
3×10⁻³
2×10⁻³
1×10⁻³
Rate (g/cm²·min)
0
2
4
6
8
Time (hours)
MUB-11116

Fig. 5

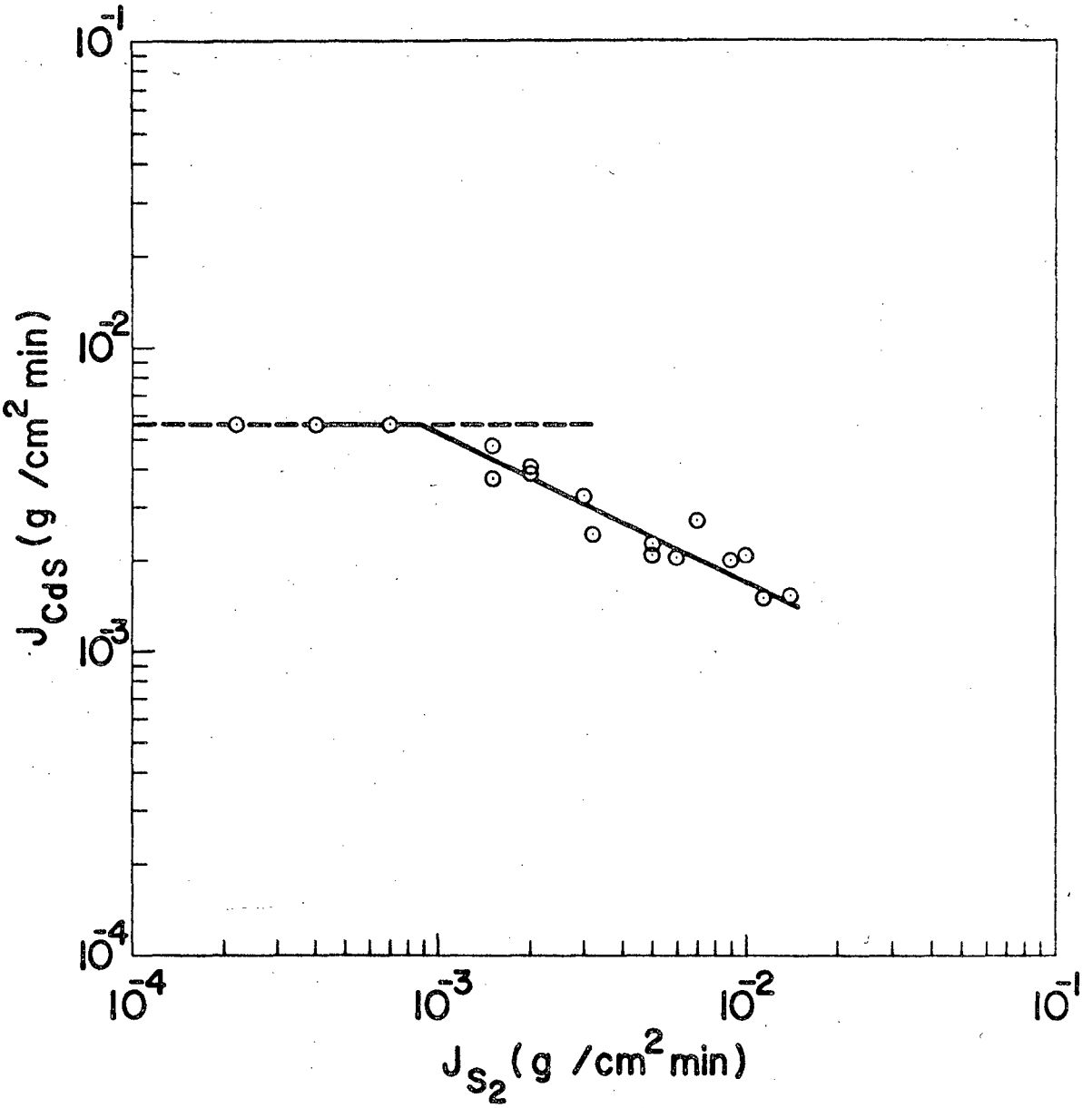
10^{-1}
10^{-2}
10^{-3}
10^{-4}
J_{CdS} (g /cm^2 min)
10^{-4}
10^{-3}
10^{-2}
10^{-1}
J_{S_2} (g /cm^2 min)
MUB-11014

Fig. 6

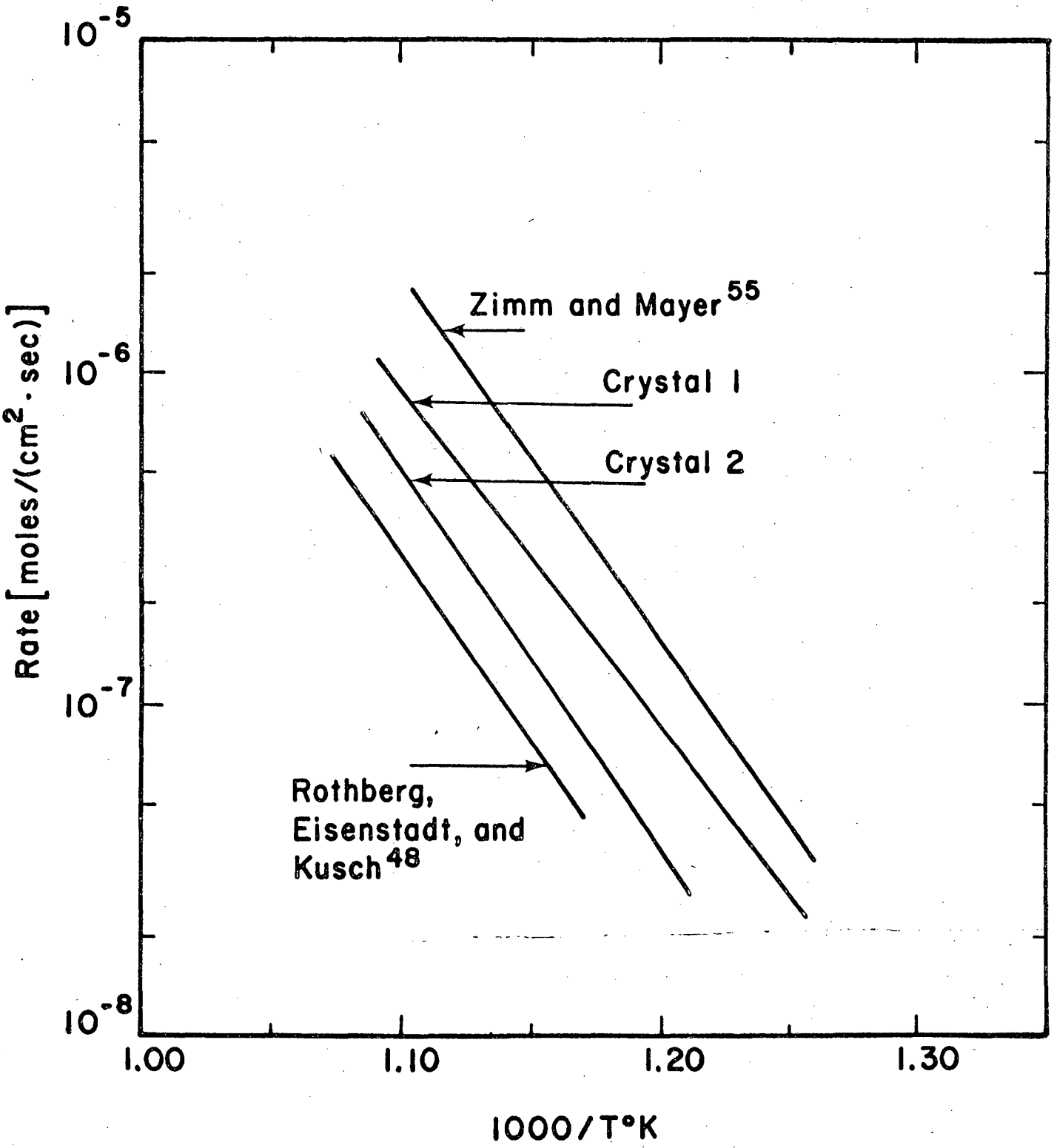
10^{-5}
10^{-6}
10^{-7}
10^{-8}
Rate [moles/(cm^2 · sec)]
Zimm and Mayer[55]
Crystal 1
Crystal 2
Rothberg, Eisenstadt, and Kusch[48]
1.00
1.10
1.20
1.30
1000/T°K

Fig. 7